Proceedings of the 9th World Congress on Momentum, Heat and Mass Transfer (MHMT 2024)
London, United Kingdom – April 11 – 13, 2024
Paper No. ICMFHT 161
DOI: 10.11159/icmfht24.161

Influence of Liquid Electrical Conductivity on the Electroosmotic Flow Characteristics inside the Wavy Microchannel under Joule Heating

Sumit Kumar Mehta[1], Pranab Kumar Mondal[1], Somchai Wongwises[2]
[1]Microfluidics and Microscale Transport Processes Laboratory
Department of Mechanical Engineering,
Indian Institute of Technology Guwahati, Guwahati-781039, Assam, India
[2]Fluid Mechanics, Thermal Engineering and Multiphase Flow Research Laboratory (FUTURE), Department of Mechanical Engineering, Faculty of Engineering, King Mongkut's University of Technology Thonburi (KMUTT), Bangmod, Bangkok 10140, Thailand
sumit090391@gmail.com

Abstract - In light of the Joule heating impact, the goal of this work is to examine how electrical conductivity affects the electroosmotic flow characteristics inside wavy microchannels. Leveraging the COMSOL Multiphysics software, thereby a numerical model has been designed to calculate the underlying temperature, potential, and flow fields. Additionally, the experimental findings in the limiting scenario validate the numerical model. Employing a range of physically logical variables for the wavy wall dimensionless amplitude, liquid's reference electrical conductivity, and reference external electric field, we deeply examined the external electric field, conductive heat lines, flow field, maximum temperature rise, and average flow velocity. Both the electroosmotic flow velocity and the conductive heat flux intensity have been identified to be more intense at bigger amplitudes of the wavy microchannel owing to the enhanced electric field strength located in the throat. An increase in the conductive heat flux intensity, which allows for an increase in the flow velocity magnitude, is brought about by an increase in the liquid's reference electrical conductivity. As the reference electrical conductivity and electric field intensity increased, it became apparent that the maximum temperature rise also increased. Nevertheless, the same reduces as the wavy wall's amplitude increases. In response to an intensification in electrical conductivity, the average flow velocity only increases when the reference electric field intensity is high, from 25000 to 50000 V/m. Moreover, as the wave amplitude expands, the flow velocity decreases. Designing an electrical force-driven flow manipulator that produces heat through Joule heating can benefit from the insights drawn from this work.

***Keywords*:** Joule heating, Electroosmotic flow, Electrical-double layer, Microchannel.

1. Introduction

An electrical double layer (EDL) in the microfluidic conduit facilitates one to regulate the flow field by manipulating the electroosmotic flow produced by the external electric field. Compared to pressure-driven flows, this form of flow offers superior controllability and manipulation abilities. Consequently, in the last decade, the scientific community has become more involved in studying electroosmotic flow manipulating devices.

Furthermore, the modulation of the microchannel's geometry allows for the development of a locally changing electrical field, which, in turn, enables the local manipulation of the electrical body force to provide corresponding flow actuation. As a result, numerous researchers have recently investigated the modulation of the electroosmotic vortex in wavy microchannels with non-uniform zeta potential [1]–[3]. Furthermore, localized perturbations in material properties are able to be achieved through the generation of heat via volumetric Joule heating, which is made possible by the introduction of an external electrical field. The Joule heating effect in straight microchannels has been analyzed through both numerical and experimental experiments [4]–[6]. These findings imply that the Joule heating effect on flow and mass transfer is typically triggered by the liquid's increased electrical conductivity.

After a thorough assessment of the literature, it became apparent that there is a lack of research in the open literature about the impact of solution electrical conductivity on the electroosmotic flow characteristics inside wavy microchannels when considering the Joule heating effect. Thus, by manipulating the electrical conductivity, applied potential difference, and wavy wall amplitude, the current work aims to investigate the flow field, external local electric field, and heat flow pattern within the wavy microchannel. Further enhancing the usefulness of the current analysis is the consideration of temperature-dependent thermophysical properties, which are very sensitive.

2. Mathematical modelling

Figure 1(a) demonstrations a schematic diagram of the wavy microchannel with a solid PDMS wall. The external electric field, which develops by introducing a potential difference of ΔV across the ends of the microchannel, drives the electroosmotic flow. The microchannel's average length is 200 μm, while its average height is 20 μm. Taking in to account the temperature dependency of highly sensitive material properties including thermal conductivity, relative permittivity, and electrical conductivity for the liquid, the relevant transport equations for the flow field, electrical double layer potential field, external potential field, and temperature are expressed mathematically.

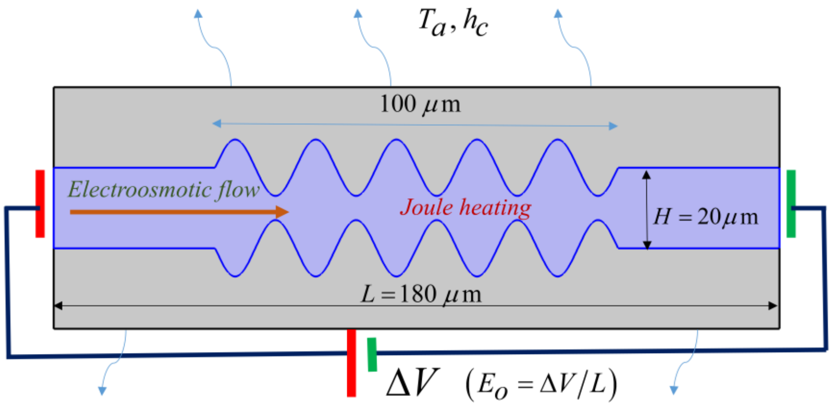

Fig. 1: Schematic depiction illustrating the wavy microchannel with PDMS solid wall.

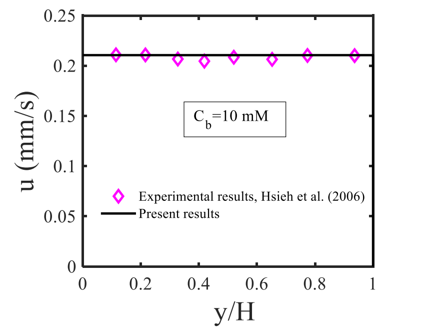

Fig. 2: The comparison of the flow velocity profile produced by this work with Hsieh et al. [9].'s findings from experimentation.

Incorporating the electrical body force for the electroosmotic flow, we obtained the flow field using the continuity and momentum transport equations:

$$\nabla \cdot \vec{\mathbf{u}} = 0 \tag{1a}$$

$$\rho\left(\vec{\mathbf{u}} \cdot \nabla\right)\vec{\mathbf{u}} = -\nabla p + \nabla \cdot [\mu_T (\nabla \vec{\mathbf{u}} + (\nabla \vec{\mathbf{u}})^{\mathrm{T}})] + \rho_e \left(\nabla\left(\phi + \psi\right)\right) \tag{1b}$$

Here, velocity vector, local pressure, temperature dependent viscosity are denoted by letters $\vec{\mathbf{u}}$, p, and μ_T, respectively. The space charge density is written as $\rho_e = -\left(2000 zeN_a C_b\right)\sinh\left(\psi ze/k_B T\right)$, viscosity as $\mu_T = 2.761\exp\left(1731/T\right)\times 10^{-6}$ Pa-s [7], density of liquid $\rho = 1000\ \mathrm{kg/m^3}$. C_b is the molar concentration.

We have solved external potential field (ϕ) and EDL potential field (ψ) using the following equation:

$$\varepsilon_0 \nabla \cdot \left(\varepsilon_{r,T} \nabla \psi\right) = \left(2000 zeN_a C_b\right)\sinh\left(\psi ze/k_B T\right) \tag{2}$$

$$\nabla \cdot \left(\sigma_T \nabla \phi\right) = 0 \tag{3}$$

Here, $\varepsilon_{r,T} = 305.7 exp\left(-T/219\right)$ [7] and electrical conductivity $\sigma_T = \sigma_o\left(1 + 0.02\left(T - 298\right)\right)\ \mathrm{S/m}$ [8]; σ_o is the reference electrical conductivity of the liquid.

Moreover, the temperature field (T) has been solved using the energy equation for liquid and solid PDMS domain as:

$$\rho c_p \left(\vec{\mathbf{u}} \cdot \nabla T\right) = -\nabla \cdot \left(k_T \nabla T\right) + \sigma_T \left|\vec{\mathbf{E}}\right|^2 \tag{4a}$$

$$0 = -\nabla \cdot \left(k_{PDMS} \nabla T\right) \tag{4b}$$

Here, thermal conductivity, $k_T = 0.61 + (1 + 0.0012(T - 298))\ \text{W/m-K}$ [8], electric field magnitude, $|\vec{\mathbf{E}}| = \sqrt{(\partial\phi/\partial x)^2 + (\partial\phi/\partial y)^2}$, constant pressure specific heat capacity, $c_p = 4180\ \text{J/kg-K}$ and $k_{PDMS} = 0.16\ \text{W/m-K}$ is the undertaken conductivity associated with the thermal transport within the PDMS material.

A zeta potential of -0.05 V, inlet and ambient temperatures of 298 K, inlet and outlet gauge pressures of 0 Pa, and a and a convective heat transfer coefficient in between the PDMS solid wall and ambient of 2.5 W/m^2-K have all been employed. Based on the reference electric field, E_o, which ranges from 10,000 V/m to 50,000 V/m, the inlet side external external potential is chosen.

3. Methodology for numerical simulation and model benchmarking

Utilizing the finite element method as a framework, the COMSOL Multiphysics software enabled us to resolve the governing transport equations. To conduct the grid-independent test, the average flow velocity for a dimensionless amplitude of 0.9 was computed, and 45,792 elements were employed in all simulations. This choice was based on the fact that the related percentage error was less than 0.1% in comparison to the highly refined mesh. In order to provide more verification for the theoretical framework, the electroosmotic flow velocity profile indicated in Figure 1(b) has been compared with the data from experiments obtained by Hsieh et al. [9]. The close comparison demonstrates that the current model is reliable.

4. Results and discussion

We systematically examined the external electric field, conductive heat lines, flow field, maximum temperature rise, and average flow velocity by varying the wavy wall dimensionless amplitude ($0 \le \alpha = A/0.5H \le 0.9$), reference electrical conductivity of the liquid (0.01 S/m $\le \sigma_o \le 1$ S/m), and reference external electric field (10000 V/m $\le E_o$ 50000 V/m) in physically justified ranges [4]–[6]. In the current situation, the amplitude of the wavy microchannel wall is represented by the letter A.

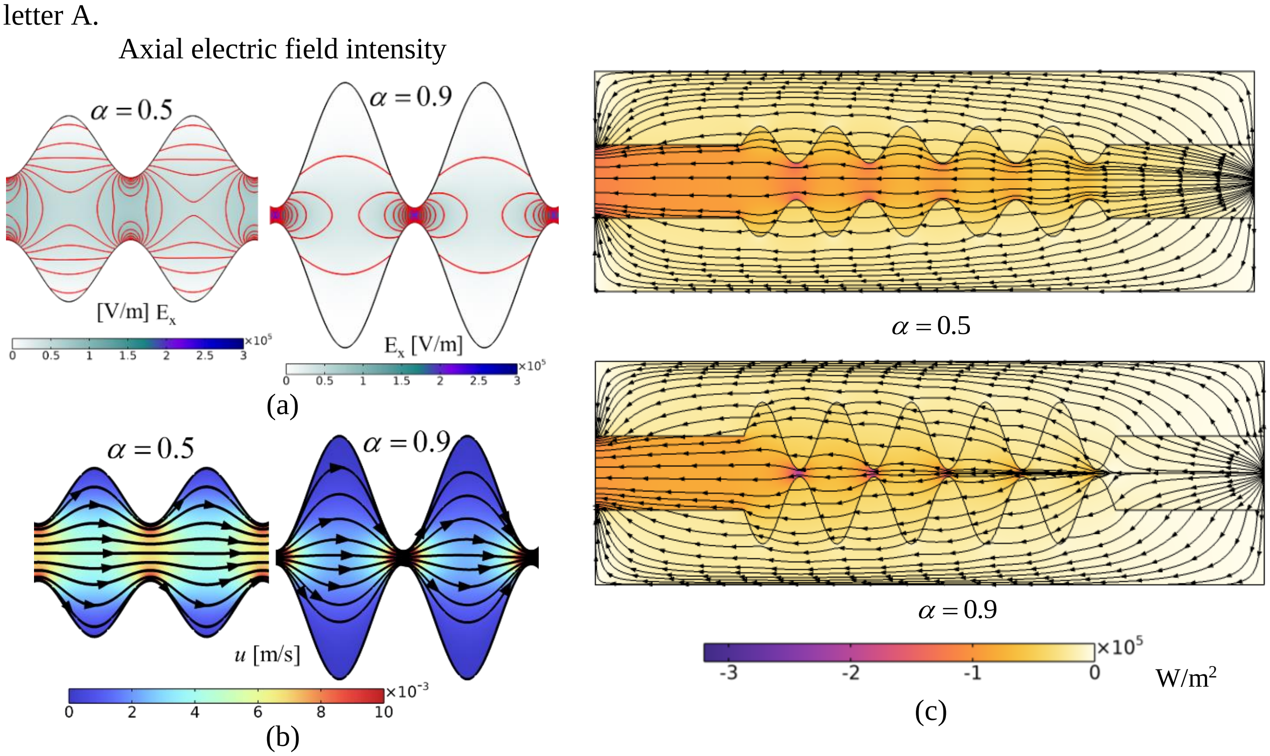

Fig. 3: (a) Contours of axial external electric field intensity, (b) flow field and streamlines and (c) conductive heat lines and its intensity for dimensionless amplitude 0.5 and 0.9 when E_o = 50000 V/m and σ_o =1 S/m.

From Fig. 3(a), we can observe that the external electric field intensity concentrates at the wavy throat and increases with increasing amplitude. This phenomenon occurs because the electric field lines are denser at the throat with a larger amplitude, allowing for a higher intensity. Consequently, Fig. 3(b) shows a higher electroosmotic flow intensity at a larger amplitude due to the larger electrical body force at the throat.

Similarly, Fig. 3(c) depicts a higher amplitude of conductive heat flux intensity due to the increased Joule heating intensity at the region of the throat. Furthermore, because the downstream side temperature is higher due to Joule heating compared to the inlet colder liquid, the conductive heat lines propagate from the right to the left.

As shown in Fig. 4(a), increasing the reference electrical conductivity from 0.01 S/m to 1 S/m can increase the flow intensity near the throat region. This effect is due to the fact that increased electrical conductivity raises the domain temperature and amplifies the intensity of Joule heating. Consequently, the increased temperature rise significantly reduces the liquid viscosity near the throat region, thereby lowering flow resistance and increasing the flow velocity intensity. For a clearer visual representation, Fig. 4(b) depicts the flow velocity at the trough region for various reference electrical conductivity values. The core flow velocity experiences a significant increase due to the reduced viscosity induced by higher electrical conductivity. Furthermore, as illustrated in Fig. 4(c), the intensity of conductive heat flow increases by an order of two when the reference electrical conductivity increases from 0.01 S/m to 0.1 S/m, owing to the increased intensity of the Joule heating term.

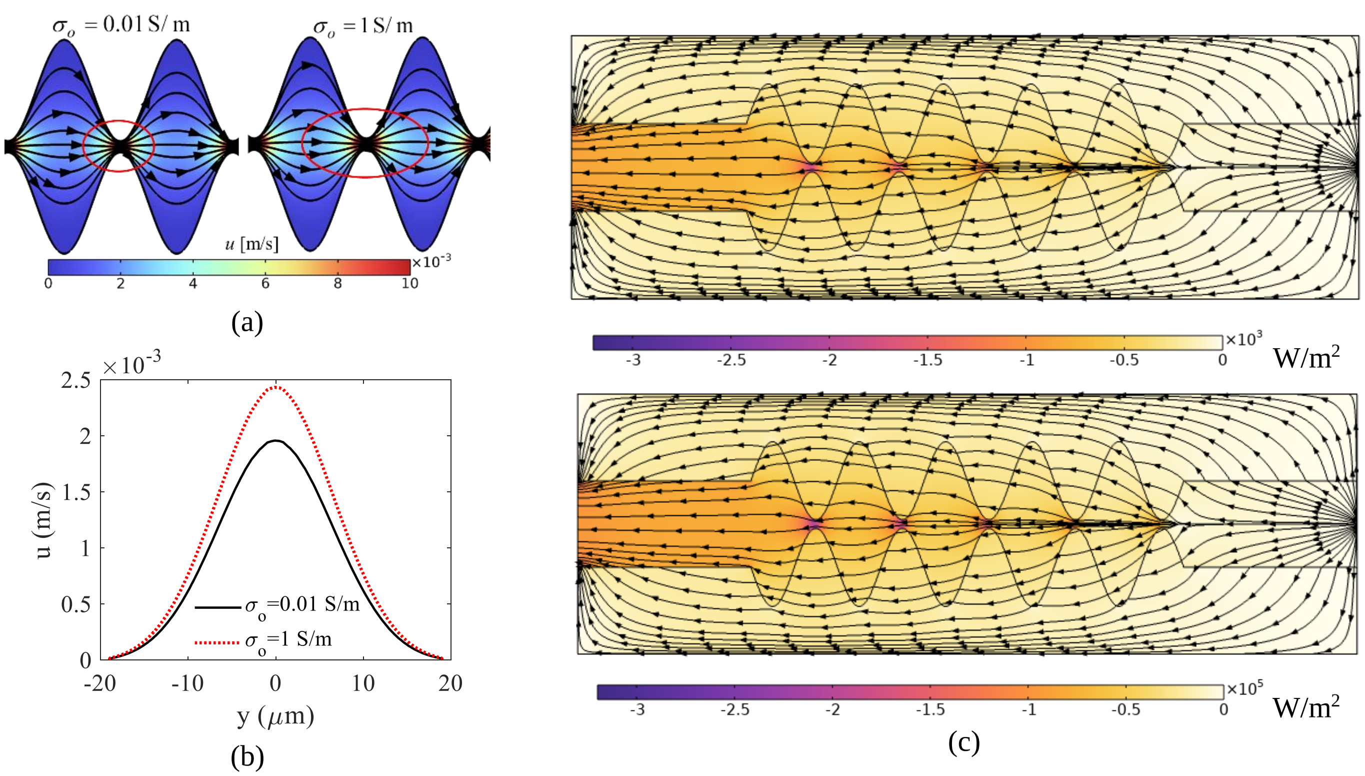

Fig. 4: (a) Contours of flow field and streamlines and (b) flow velocity profile at trough section of wavy microchannel and (c) conductive heat lines and its intensity for reference electrical conductivity 0.01 and 1 S/m when 0.5 E_o = 50000 V/m and dimensionless amplitude is 0.9.

The internal temperature rise of any microfluidic device is of tremendous relevance since it affects the degradation of species associated with that flow. Fig. 5(a) shows the maximum temperature rise in the liquid domain resulting from the variation in the reference electrical conductivity at various reference electric field values. Due to the less pronounced increase in volumetric Joule heating at 10,000 V/m, we can observe that the maximum temperature rise is milder with an increase in reference electrical conductivity. However, with a reference electrical conductivity of 1 S/m, significant enhancements of up to 18.6 K are possible, attributable to the substantial increases in Joule heating at higher electrical conductivity for 50,000 V/m.

Furthermore, as depicted in Fig. 5(b), the maximum temperature can be lowered owing to the smaller area of stronger electric field strength at greater amplitude (as shown in Fig. 3(a)). Consequently, wavy walls, resulting in a lower temperature rise, may be beneficial for the flow of biological species.

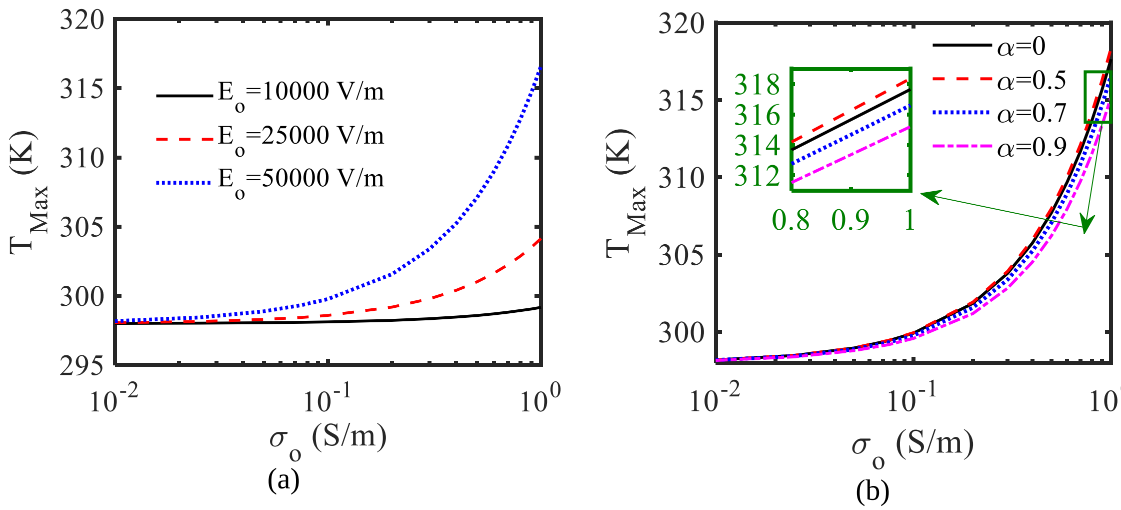

Fig. 5: Plot of the maximum temperature rise (T_{Max}) with change in reference electrical conductivity at different (a) reference electric field intensity and (b) at the different values of dimensionless amplitude of the wavy wall.

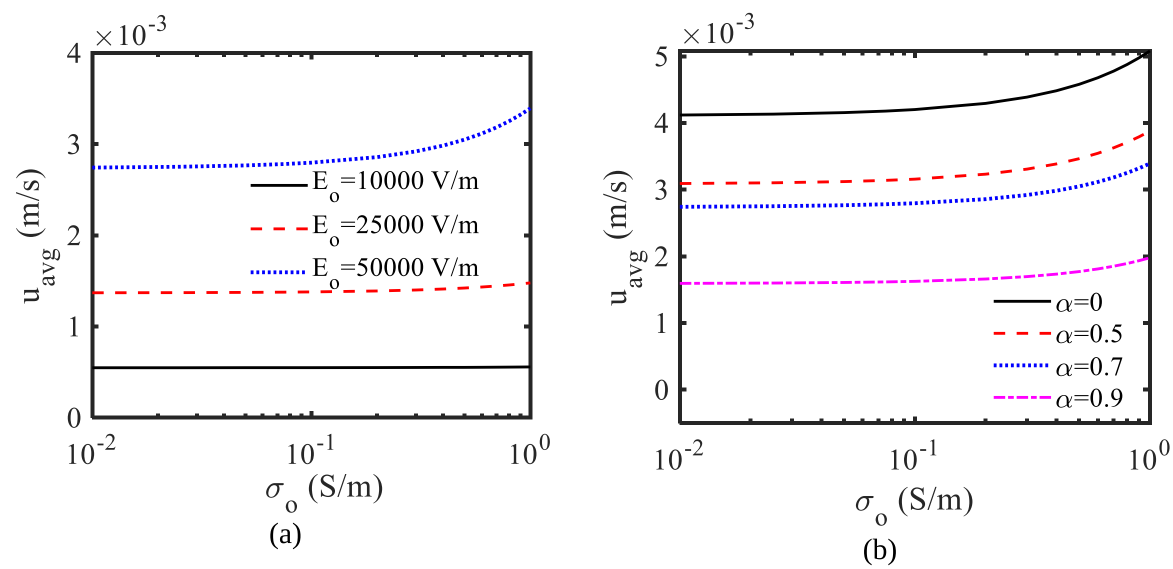

Fig. 6: Plot of the average flow velocity (u_{avg}) with change in reference electrical conductivity at different (a) reference electric field intensity and (b) at the different values of dimensionless amplitude of the wavy wall.

We now present the associated mass transport under electroosmotic actuation in a wavy microchannel in terms of average flow velocity with respect to the variation in reference electrical conductivity at varying intensities of the reference electric field in Fig. 6(a). Due to the minor temperature rise at 10,000 V/m, as illustrated in Fig. 5(a), we find that the average flow velocity is almost insensitive to an increase in reference electrical conductivity. Conversely, at greater intensities of the external electric field (e.g., 50,000 V/m), where the maximum temperature rise is more intensive (Fig. 5(a)), the viscosity is significantly reduced, leading to a substantial increase in the average flow velocity. Additionally, as shown in Fig. 6(b), when the amplitude of the wavy wall increases, the average flow velocity decreases due to the rise in flow resistance and the narrower region of increased electrical field intensity (as seen in Fig. 3(a)) at a larger amplitude.

5. Conclusion

By systematically varying the wavy wall dimensionless amplitude, reference electrical conductivity of the liquid, and reference external electric field within physically justified ranges, we conducted a thorough investigation of the external electric field, conductive heat lines, flow field, maximum temperature rise, and average flow velocity. The following summarizes the most significant findings of the current work:

- Both the electroosmotic flow velocity and the conductive heat flux intensity are higher at greater amplitudes of the wavy microchannel due to the increased electric field intensity at the throat.
- An increase in the liquid's reference electrical conductivity leads to a significant rise in the conductive heat flux intensity, which in turn allows for an increase in the magnitude of the flow velocity.
- It was observed that the maximum temperature rise increases with the reference electrical conductivity and electric field intensity. However, this rise decreases as the amplitude of the wavy wall increases.
- The average flow velocity only increases when the reference electric field intensity is high, between 25,000 and 50,000 V/m, in response to an increase in electrical conductivity. Additionally, the flow velocity decreases as the amplitude of the wavy wall increases.

References

[1] S. K. Mehta and S. Pati, “Enhanced Electroosmotic Mixing in a Wavy Micromixer Using Surface Charge Heterogeneity,” *Ind. Eng. Chem. Res.*, Feb. 2022, doi: 10.1021/acs.iecr.1c04318.

[2] A. Banerjee, A. K. Nayak, A. Haque, and B. Weigand, “Induced mixing electrokinetics in a charged corrugated nano-channel: towards a controlled ionic transport,” *Microfluid. Nanofluidics*, vol. 22, no. 10, p. 115, 2018, doi: 10.1007/s10404-018-2128-3.

[3] S. K. Mehta, B. Mondal, S. Pati, and P. K. Patowari, “Enhanced electroosmotic mixing of non-Newtonian fluids in a heterogeneous surface charged micromixer with obstacles,” *Colloids Surfaces A Physicochem. Eng. Asp.*, vol. 648, p. 129215, 2022, doi: https://doi.org/10.1016/j.colsurfa.2022.129215.

[4] S. Sridharan, J. Zhu, G. Hu, and X. Xuan, “Joule heating effects on electroosmotic flow in insulator-based dielectrophoresis,” *Electrophoresis*, vol. 32, no. 17, pp. 2274–2281, 2011, doi: 10.1002/elps.201100011.

[5] G. Y. Tang, C. Yang, J. C. Chai, and H. Q. Gong, “Joule heating effect on electroosmotic flow and mass species transport in a microcapillary,” *Int. J. Heat Mass Transf.*, vol. 47, no. 2, pp. 215–227, 2004, doi: 10.1016/j.ijheatmasstransfer.2003.07.006.

[6] X. Xuan, B. Xu, D. Sinton, and D. Li, “Electroosmotic flow with Joule heating effects,” *Lab Chip*, vol. 4, no. 3, pp. 230–236, 2004, doi: 10.1039/B315036D.

[7] G. Y. Tang, C. Yang, J. C. Chai, and H. Q. Gong, “Joule heating effect on electroosmotic flow and mass species transport in a microcapillary,” *Int. J. Heat Mass Transf.*, vol. 47, no. 2, pp. 215–227, 2004, doi: https://doi.org/10.1016/j.ijheatmasstransfer.2003.07.006.

[8] S. Sánchez, G. Ascanio, F. Méndez, and O. Bautista, “Theoretical analysis of non-linear Joule heating effects on an electroosmotic flow with patterned surface charges,” *Phys. Fluids*, vol. 30, no. 11, p. 112002, Nov. 2018, doi: 10.1063/1.5051175.

[9] S. S. Hsieh, H. C. Lin, and C. Y. Lin, “Electroosmotic flow velocity measurements in a square microchannel,” *Colloid Polym. Sci.*, vol. 284, no. 11, pp. 1275–1286, 2006, doi: 10.1007/s00396-006-1508-5.